GLAST's GBM Burst Trigger

D. Band*, M. Briggs†, V. Connaughton†, M. Kippen** and R. Preece†

*Code 661, NASA/Goddard Space Flight Center, Greenbelt, MD 20771
†National Space Science and Technology Center, Huntsville, AL 35805
**NIS-2, Los Alamos National Laboratory, Los Alamos, NM 87545

Abstract. The GLAST Burst Monitor (GBM) will detect and localize bursts for the GLAST mission, and provide the spectral and temporal context in the traditional 10 keV to 25 MeV band for the high energy observations by the Large Area Telescope (LAT). The GBM will use traditional rate triggers in up to three energy bands, and on a variety of timescales between 16 ms and 16 s.

THE MISSION

The Gamma-ray Large Area Space Telescope (GLAST) is the next NASA general gamma-ray astrophysics mission, which is scheduled to be launched into low Earth orbit in February, 2007, for 5–10 years of operation. It will consist of two instruments: the Large Area Telescope (LAT) and the GLAST Burst Monitor (GBM). A product of a NASA/DOE/international collaboration, the LAT will be a pair conversion telescope covering the $<$20 MeV to $>$300 GeV energy band. The LAT will be $\sim$30 times more sensitive than *CGRO's* EGRET.

The GBM will detect and localize bursts, and extend GLAST's burst spectral sensitivity to the $<$10 keV to $>$25 MeV band. Consisting of 12 NaI(Tl) (10–1000 keV) and 2 BGO (0.15–25 MeV) detectors, the GBM will monitor $>$8 sr of the sky, including the LAT's field-of-view (FOV). Bursts will be localized to $< 15^\circ$ (1σ) by comparing the rates in different detectors.

During most of the mission GLAST will survey the sky by rocking $\sim 35^\circ$ above and below the orbital plane around the zenith direction once per orbit. The first year will be devoted to a sky survey while the instrument teams calibrate their instruments. During subsequent years guest investigators may propose pointed observations, but continued survey mode is anticipated because it will usually be most efficient.

Both the GBM and the LAT will have burst triggers. When either instrument triggers, a notice with a preliminary localization will be sent to the ground through TDRSS and then disseminated by GCN. Additional data will be sent down through TDRSS for an improved rapid localization on the ground. "Final" positions will be calculated from the full downlinked data. All positions will be disseminated as GCN Notices, and additional information (e.g., fluences and durations) will be sent out as GCN Circulars.

Using its own and the GBM's observations, the LAT will decide autonomously whether to slew to the burst location for a 5 hour followup pointed observation. The threshold will be higher for GBM-detected bursts outside the LAT's FOV.

The GBM's NaI and BGO detectors will provide the number of counts detected in

8 energy bands every 16 ms; the GBM will trigger off these rates. Rate triggers test whether the increase in the number of counts in an energy band ΔE and time bin Δt is statistically significant; the expected number of non-burst photons in the ΔE–Δt bin is estimated by accumulating counts before the time bin being tested. Building on our experience with the BATSE trigger, we are performing trade studies to optimize the sensitivity of these triggers. Here we present the results of our studies focusing on the choice of ΔE and Δt.

CHOICE OF ΔT

We consider two Δt hierarchies—Δt spaced by factors of $\times 2$ (e.g., 16 ms, 32 ms, 64 ms...) or $\times 4$ (e.g., 16 ms, 64 ms, 256 ms...)—and three time bin registrations—non-overlapping bins (e.g., bins separated by 1024 ms for Δt=1024 ms bins), half-step bins (e.g., bins separated by 512 ms for Δt=1024 ms bins), and all possible bins (e.g., bins every 16 ms). Varying Δt can maximize the signal-to-noise ratio, while more time registrations permit the bin to be centered over the peak flux, also maximizing the signal-to-noise ratio. To test these 6 triggers we applied them to the 64 ms resolution lightcurves of the 25 brightest BATSE bursts; for each lightcurve we chose 10 starting times at random. Note that the GBM rates will have 16 ms resolution.

The most sensitive trigger would have Δt spaced by $\times 2$ and every possible time bin. The next most sensitive trigger would have Δt spaced by $\times 2$ and bins spaced every half step. These triggers would test different numbers of bins—11264 bins vs. 3070 bins tested every 16.384 s.

Besides the increased computational burden, the risk of a false trigger increases as the number of bins tested increases, but the false trigger probability is not proportional to the number of bins because the bins are not independent. Our simulations indicate this is a $<$5% effect—for the same false trigger rate the trigger threshold should be raised by a few percent as the number of time bins tested increases.

CHOICE OF ΔE

Triggering on the counts accumulated in different ΔE can tailor the detector sensitivity to hard or soft bursts. The GBM will be able to trigger on more than one ΔE, and therefore we seek the set that will maximize the sensitivity for both hard and soft bursts, although hard bursts are a priority since their spectra are more likely to extend into the LAT's energy band (of course one must be careful of one's theoretical prejudices). For the study of detector sensitivity to different types of bursts and for comparisons between detectors, the F_T-E_p plane is useful[1], where F_T is the peak photon flux in a fiducial energy band (here 1–1000 keV) and E_p is the energy of the peak of $E^2N(E) \propto \nu f_\nu$. Burst spectra are also characterized by asymptotic low and high energy power laws with spectral indices α and β, respectively; the dependence of F_T on α and β is not as great as on E_p. For a given set of spectral indices the detector sensitivity (the threshold value of F_T at a give E_p) is a curve in the F_T-E_p plane.

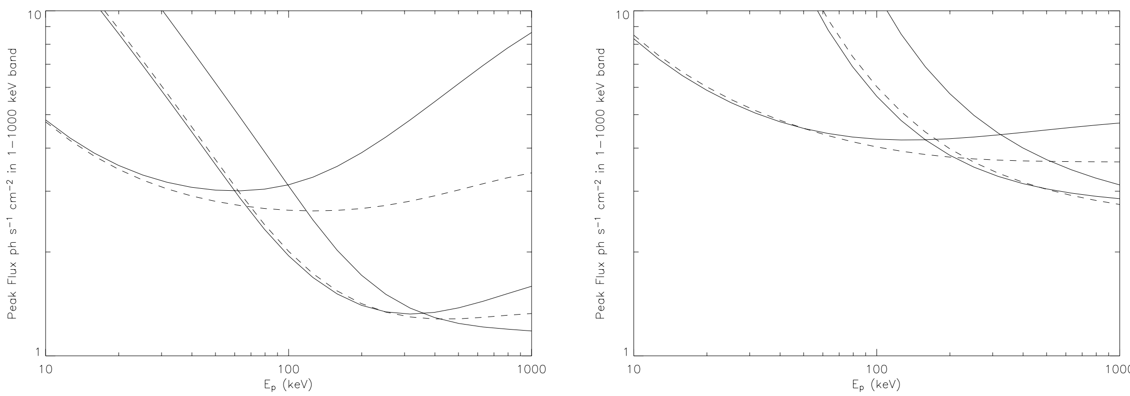

FIGURE 1. Sensitivity for two sets of ΔE for α=0, $\beta = -2$ (left plot) and $\alpha = -1$, $\beta = -25$ (right plot). The solid curves are for (left to right within plot) ΔE=5–100, 50–300 and 100–1000 keV and the dashed for ΔE=5–1000 and 50–1000 keV. Lower curves are more sensitive.

To calculate these sensitivity curves we need both the number of counts a detector will detect in the nominal ΔE band for a given burst spectrum and the number of background counts in this ΔE. A code has been developed to calculate these numbers for each GBM detector for a burst in any direction relative to the spacecraft. Currently the code uses response matrices for the flux directly incident on the detectors (without scattering off the spacecraft or the Earth, but with obscuration by other parts of the observatory), and a model of the background on orbit. We used this code to calculate the sensitivity along the normal to the LAT for Δt=1.024 s assuming at least two detectors trigger at $\sigma_0 > 5.5$.

We calculated the sensitivity curves for a variety of ΔE. The extremes of our spectral index sets were α=0, $\beta = -2$ and $\alpha = -1$, $\beta = -25$. The first set is similar to the spectra sometimes observed early in a burst; its high energy tail would be more easily detected by the LAT. The second set is a spectrum without a high energy tail.

Figure 1 shows the sensitivity for two sets of ΔE. To compare the GBM and BATSE burst distributions we would like to include ΔE=50–300 keV, which was BATSE's primary trigger band. As can be seen, ΔE with a low energy cutoff of $\sim$50 keV is optimal for high energy sensitivity because it does not include the large low energy background. Conversely, ΔE should always extend to the highest energy possible because of the low background at high energy.

We find that triggering a single BGO detector with $\sigma_0 = 8$ increases the sensitivity for $E_p > 1$ MeV for α=0, $\beta = -2$. There is no increase in sensitivity for $\alpha = -1$.

Figure 2 compares the Δt=1 s sensitivity for the GBM (solid) and BATSE (dot-dashed) with the burst intensity (dashed) that when the spectrum is extrapolated to the LAT energy band would result in 25 detected photons per second. The burst is assumed to be on the LAT normal, $\alpha = -1$, $\beta = -2$, and the GBM triggers on ΔE=5–100 and 50–300 keV.

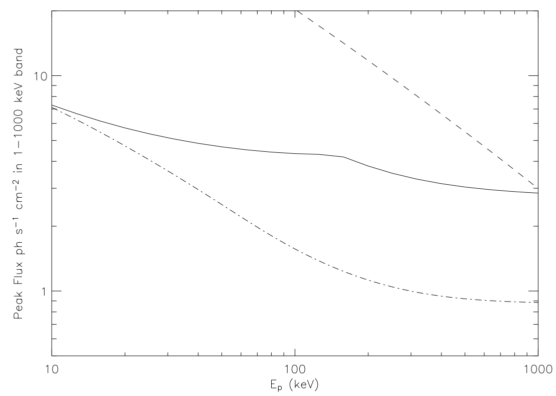

FIGURE 2. Comparison of GBM (solid curve) and BATSE (dot-dashed) sensitivities, and the flux necessary for a LAT detection of 25 photons (dashed).

CONCLUSIONS

The Δt calculations suggest that spacing Δt by factors of $\times 2$ (i.e., 16 ms, 32 ms, 64 ms...) and staggering the bins by half a timestep (e.g., the 1024 ms bins are accumulated every 512 ms) would be particularly efficient given the number of time bins that would be tested. Choosing two triggers with ΔE starting at 5 keV and 50 keV and extending to the detector's high energy cutoff would provide good high and low energy sensitivity. Using ΔE=50–300 keV would reproduce the BATSE trigger, but would reduce the $E_p > 500$ keV sensitivity for the hardest bursts (which are more likely to have LAT flux); this can be mitigated by adding ΔE=100–1000 keV.

Future trade studies will focus on the methodology for measuring the background. GLAST will slew more frequently than *CGRO* did, and therefore the background rates in GLAST's different detectors will probably vary more rapidly. We will need to suppress spurious triggers resulting from variations in the background without a major reduction in the GBM's sensitivity.

Ultimately the trigger design will be constrained by the computational capabilities of the GBM's processor.

REFERENCES

1. Band, D., *Burst Populations and Detector Sensitivity*, in these proceedings (2004).